

## Determination of Molecular Orientational Order in Cold-Stretched Poly(*p*-phenylene vinylene) Thin Films by DECODER <sup>13</sup>C NMR

Michelle L. Kropewnicki,<sup>\*1</sup> Dieter J. Schaefer,<sup>\*</sup> Manfred Hehn,<sup>†</sup> Wim Dermaut,<sup>‡</sup> Herman J. Geise,<sup>‡</sup> and Bradley F. Chmelka<sup>\*2</sup>

<sup>\*</sup>Department of Chemical Engineering, University of California, Santa Barbara, California 93106;

<sup>†</sup>Max-Planck-Institut für Polymerforschung, Postfach 3148, D-55021 Mainz, Germany; and

<sup>‡</sup>Department of Chemistry, Structural Chemistry Group, Universitaire Instelling Antwerpen (UIA), Universiteitsplein 1, 2610 Wilrijk, Belgium

FESTSCHRIFT IN HONOR OF PROFESSOR HANS-WOLFGANG SPIESS ON  
THE OCCASION OF HIS 60TH BIRTHDAY

The properties of poly(*p*-phenylene vinylene) (PPV) films depend on the degree of orientational order present in the films. Recently, Dermaut *et al.* reported a novel cold-stretching technique (*Macromolecules* **33**, 5634–5637 (2000)) in which chain alignment can be introduced into PPV precursor films by uniaxially stretching them prior to the thermal elimination reaction that forms PPV. The two-dimensional direction exchange with correlation for orientation-distribution evaluation and reconstruction (DECODER) <sup>13</sup>C NMR technique was applied to both unstretched PPV films and PPV films that were uniaxially cold stretched to a draw ratio  $\lambda = l/l_0 = 5$ . The unstretched films were found to be moderately ordered, comprised of a component present at 80% with a Gaussian distribution of 60° fwhm, while the remaining 20% is isotropically distributed. A distribution of  $9^\circ \pm 3^\circ$  fwhm was measured by NMR in good agreement with IR dichroism measurements for the uniaxially cold-stretched films, establishing that a high degree of orientational order can be introduced by cold stretching PPV films. © 2002 Elsevier Science (USA)

### 1. INTRODUCTION

The conductivity of doped and stretched poly(*p*-phenylene vinylene) (PPV) films, which are widely used in applications such as light-emitting diodes (LEDs) [1, 2], photovoltaic cells [3], and polymer-based lasers [4, 5], is directly related to the degree of orientational alignment of the molecular chains with respect to the film draw direction [6]. In highly oriented PPV, the conductivity along the draw direction can reach values as high as  $10^4$  S/cm and can be as much as 100 times the conductivity in the transverse direction [7, 8].

Films of high-molecular-weight PPV are synthesized from a water-soluble precursor polyelectrolyte, such as poly(*p*-xylylidene tetrahydrothiophenium chloride), which is converted to PPV by a thermal- or base-induced elimination reaction

<sup>1</sup>Current address: DuPont Experimental Station, E356, Wilmington, Delaware 19880-0356.

<sup>2</sup>To whom correspondence should be addressed. Fax: 805-893-4731. E-mail: bradc@engineering.ucsb.edu.



[9, 10]. If a high degree of orientational order is desired, precursor films must be uniaxially stretched before complete conversion to PPV. Until recently, oriented PPV films were prepared almost exclusively by the so-called hot stretching, that is, stretching during the thermal elimination reaction, while the products of the thermal elimination reaction, such as hydrogen chloride and tetrahydrothiophene for the reaction above, act as plasticizing agents that mitigate tearing [11, 12]. The hot-stretching process results in PPV films that possess high degrees of orientational alignment of chain axes along the draw direction, in addition to a significant amount of axial translational disorder between chains, due to paracrystallinity [11–23].

Recently, Dermaut *et al.* reported the preparation of orientationally ordered PPV films that were cold stretched prior to the thermal elimination reaction, using water vapor to plasticize the precursor polymer [11]. This preparation procedure is easier to perform and is also less dependent on factors such as film thickness and aging than the typical hot-stretching technique. Previously, Massardier *et al.* have reported that swelling of the precursor polymer, in this case poly(*p*-xylylidene tetrahydrothiophenium chloride), with methanol allowed stretching at room temperature prior to the elimination reaction [17]. This particular cold-stretching technique, however, produced PPV films with lower orientational order than films prepared by hot stretching. In contrast, infrared dichroism measurements showed that PPV films cold stretched, while swollen with water vapor, resulted in PPV films with high degrees of orientational order; the distribution of chain axes around the draw direction was measured to be 10.5° full-width-at-half-maximum (fwhm) for a draw ratio  $\lambda = l/l_0 = 5$  [11]. It is interesting to note that for low stretch ratios ( $\lambda \cong 2$ ), cold stretching of PPV films plasticized with water vapor led to higher degrees of alignment than hot stretching the films to the same draw ratio [24]. This is attributed to the onset of the elimination reaction during the early stages of hot stretching, which results in the formation of partially eliminated and therefore rigid PPV regions early in the process. If these more rigid domains are not already oriented in the direction of stretching, it may be more difficult to align them along the stretch direction later on. By contrast, in cold stretching, the elimination reaction is not initiated until after the films have been stretched and thus oriented, leading to higher degrees of PPV chain alignment [11].

The purpose of this study is to quantify molecular orientation distributions in cold-stretched PPV films, by applying the solid-state direction exchange with correlation for orientation-distribution evaluation and reconstruction (DECODER) NMR technique [25, 26]. This method can access both crystalline and amorphous regions of polymer films (like IR dichroism, though unlike X-ray scattering). The DECODER method is an extension of an earlier experiment first introduced by Henrichs [27], which applied a discrete macroscopic reorientation of a sample to determine orientation distribution moments for films of poly(ethylene terephthalate) (PET) [27]. DECODER NMR extends Henrichs's approach to include reconstruction of the orientation distribution and has been implemented to study orientational order in deuterated polyethylene films [25], PET films and fibers [28], and high tensile strength fibers of poly(*p*-phenyleneterephthalamide) [29].

Many techniques have been used to characterize the degree of orientational order, that is, the degree of alignment of the polymer chains with respect to the primary

order direction of the PPV film, which in the case of uniaxially stretched films is given by the draw direction. The key concept for specifying the molecular order in uniaxially oriented polymers is the orientation distribution function  $P(\phi_M)$ , where  $\phi_M$  represents the Euler angle that specifies the orientation of the molecular chain axis with respect to the draw direction [30]. As this orientation distribution function depends only on a single angle, it can be conveniently expanded in terms of Legendre polynomials  $P_L(\cos(\phi_M))$ , and the expansion coefficients  $\langle P_L \rangle$  reported as order parameters or moments of the orientation distribution [26, 30]. X-ray diffraction studies [12–17] have yielded values of the Hermans orientation function, which is equivalent to the second moment of the orientation distribution function,  $\langle P_2 \rangle$ , of chains around the draw direction, of up to 0.99 for a draw ratio  $\lambda = 5$  (which has, inconsistently, also been reported as an angular half-width-at-half-maximum of the X-ray intensity distribution of  $8^\circ \pm 1^\circ$ ) [15]. Gagnon *et al.* showed that the value of the Hermans orientation function increases rapidly with the draw ratio until a limiting value of  $\lambda$  was reached [13]<sup>3</sup>.

Electron microscopy studies have confirmed a high degree of orientational order in highly stretched PPV films. In such films, the Hermans orientation function ranged from 0.94 to 0.99, and the maximum deviation between fibers and the direction of stretching was found to be approximately  $9^\circ$  [16, 20, 21].

Infrared dichroic ratio measurements of the main infrared-active modes in PPV films prepared with a draw ratio  $\lambda = 5$  yielded values for the Hermans orientation function of 0.90 [13], 0.94 [15], and 0.96 [20]. Despite demonstrating the same general trends, however, the values for the Hermans orientation distribution function, as determined from infrared dichroic ratios, are lower than those obtained from X-ray measurements. This difference may be due to the biased sensitivity of X-ray measurements toward crystalline and well-ordered regions.

Using  $^2\text{H}$  NMR line shape analyses, the Hermans orientation distribution function obtained from aligned and deuterated PPV films ranged from 0.84 for a draw ratio of 2 to 0.86 for a draw ratio of 6. All segments within the stretched PPV films were found to have high degrees of orientational order [23].

In addition to the degree of orientational order, the methods mentioned above have also been used to characterize the degrees of crystallinity in highly stretched PPV films. The lateral packing of PPV polymer chains is very regular within individual PPV crystallites [14]. Electron diffraction studies have shown that PPV has a paracrystalline structure with a monoclinic unit cell [18, 20, 31]. Paracrystallinity describes systems that possess imperfect crystalline order [32], so that although the molecular chains exhibit high degrees of alignment along the stretch axis, they show significant axial translational disorder [18]. Axial translational disorder means that there is no preferred orientation between different chains; in other words, the phenyl rings on adjacent chains do not preferentially align with each other.

In one study [16], dark-field TEM revealed that approximately half of the sample volume consisted of highly ordered crystalline domains, while the remainder

<sup>3</sup>In that study, the Hermans orientation function was approximated as  $1/2(3 \cos^2 \langle \theta \rangle - 1)$  (instead of the exact integral method of calculating the cosine average  $\langle P_2 \rangle = 1/2 \langle 3 \cos^2 \theta - 1 \rangle = 1/2 (3 \langle \cos^2 \theta \rangle - 1)$ ), where the average angle  $\langle \theta \rangle$  was taken to be the full angular width at half the maximum of the intensity distribution of the reflection.

consisted of grain boundary regions. It was not possible to determine the degrees of alignment within the disordered grain boundary regions, because the disordered PPV chains could not be directly observed by this method. However, the rigidity of the PPV chains most likely rules out a truly amorphous phase in these regions; instead, a relatively disordered state with no long-range periodicity is expected for the chains in the grain boundary regions [16]. In addition, the good mechanical properties of PPV reflect a high level of intermolecular connectivity [33], such as would be provided by molecules bridging between crystallites. Oriented PPV can thus be considered a network of highly connected crystallites [16]. The high-volume fraction of disordered grain boundary regions observed indicates that a method that can measure contributions from both crystalline and non-crystalline regions, such as NMR, would be most appropriate to characterize the orientational order in highly stretched PPV films. In contrast, X-ray diffraction studies may not accurately capture the orientational order in highly stretched PPV films, as they are inherently biased toward scattering intensity from highly ordered crystalline regions.

## 2. EXPERIMENTAL

### 2.1. Sample Preparation

Cold-stretched and unstretched PPV films were prepared as described in detail elsewhere [11]. To meet sample geometry constraints imposed by the home-built DECODER NMR probehead, PPV films were cut into pieces approximately 6 mm long, then stacked carefully by hand to align the primary order direction of the films. It is estimated that the error introduced by misalignment of the films is less than  $\pm 5^\circ$ . After stacking, the films were secured as bundles, and fixed firmly in a sample holder with the draw direction aligned in the desired orientation. To obtain spectra from samples with an isotropic orientation distribution, which are commonly referred to as “powder” samples in NMR, unstretched films were cut into pieces approximately 1 mm  $\times$  1 mm and packed randomly in an NMR tube.

### 2.2. DECODER Data Acquisition and Processing

All NMR experiments were performed at room temperature on a Chemagnetics spectrometer operating with a  $^1\text{H}$  frequency of  $2\pi \times 180$  MHz and a carbon frequency of  $2\pi \times 45.3$  MHz. The recycle delay used in the DECODER experiments was 2 s, the  $^{13}\text{C}$   $90^\circ$  pulsewidth was approximately 6  $\mu\text{s}$ , and 1 ms was used as a CP contact time. A homebuilt,  $^{13}\text{C}$ - $^1\text{H}$  double-resonance DECODER NMR probehead with a 1-cm-diameter rf-coil was used. The DECODER probehead has a wheel situated so that it holds the sample within the rf-coil. A Kevlar<sup>®</sup> string is secured on the wheel and moves freely through the body of the probe. This string connects to another Kevlar<sup>®</sup> string, which is secured to a similar wheel connected to the shaft of a precision stepping motor, which was computer controlled and synchronized with the pulse program to move the sample by

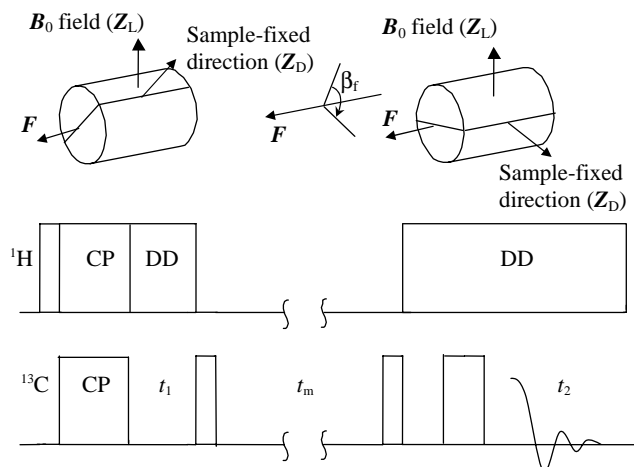


**FIG. 1.** Pulse sequence for acquisition of 2D DECODER  $^{13}\text{C}$  NMR spectra. While the sample is in the starting position, cross-polarization from  $^1\text{H}$  to  $^{13}\text{C}$  is induced. During the evolution period,  $t_1$ , which is incremented to create the two-dimensional spectrum, high-power dipolar decoupling is applied. At the end of the evolution period, a  $90^\circ$  pulse is applied to store one component of the magnetization along the  $z$ -axis. During the subsequent mixing time,  $t_m$ , the sample is flipped through an angle  $\beta_f$  about the flip axis  $F$ , which is oriented perpendicular to the external magnetic field  $B_0$ . To acquire the dead-time-free signal during the detection period  $t_2$ , a spin echo sequence is applied. During the relaxation delay, the sample is returned to its original position and the sequence repeated.

the flip angle,  $\beta_f$ . When the stepping motor shaft turns, the sample is rotated through the same number of degrees.

Figure 1 shows the pulse sequence of the DECODER NMR technique as applied to natural abundance  $^{13}\text{C}$  with cross-polarization from  $^1\text{H}$ . DECODER is a two-dimensional (2D) exchange experiment with macroscopic reorientation of a solid sample around the rotation or flip axis,  $F$ , by a discrete angle  $\beta_f$  during the mixing time  $t_m$ . The sample is initially oriented at angles  $(\alpha_1, \beta_1)$  with respect to the  $B_0$  field,  $\alpha$  and  $\beta$  being the azimuthal and polar angles of the  $B_0$  field in a sample fixed coordinate system (see below). The  $^{13}\text{C}$  spins are excited by cross-polarization from the protons and precess for the evolution time,  $t_1$ . Then, a  $90^\circ$  pulse is applied to store one component of the magnetization along the  $Z_L$ -axis. The sample is then flipped during the mixing time,  $t_m$ , to a new orientation,  $(\alpha_2, \beta_2)$ , relative to  $B_0$ ; at this new orientation the signal is detected during a time  $t_2$  with a spin echo sequence. During the recycle delay, the sample is returned to its original orientation, so that extended signal averaging can be implemented. Flip times were approximately 300 ms for a  $90^\circ$ -sample flip. For most of the DECODER experiments, 40  $t_1$  increments of either 20 or 24  $\mu\text{s}$  were acquired; the excitation frequency-offsets in  $t_1$  and  $t_2$  are chosen to lie outside the range of NMR frequencies observed in the PPV spectrum, so that only one time domain data signal needs to be acquired. The pure absorption mode 2D frequency domain spectrum is then generated by two successive Fourier transformations; the identical mirror image spectrum resulting from the

cosine transformation is discarded:

$$S(\omega_1, \omega_2) \approx \iint \langle \cos[i\omega(\vartheta_1, \varphi_1)t_1] \exp[i\omega(\vartheta_2, \varphi_2)t_2] \rangle \exp(-i\omega_1 t_1) \\ \times \exp(-i\omega_2 t_2) dt_1 dt_2,$$

where the angle brackets  $\langle \rangle$  represent an ensemble average over all possible values of  $\vartheta$  and  $\varphi$ . The observed spectral intensity  $S(\omega_1, \omega_2)$  represents the probability that a molecular segment will have a frequency  $\omega(\vartheta_1, \varphi_1)$  before the sample reorientation and a frequency  $\omega(\vartheta_2, \varphi_2)$  afterwards;  $\vartheta$  and  $\varphi$  are the polar angles of the external magnetic field in the principal axis system of the NMR interaction tensor (see below) [4]. A conventional 2D exchange experiment performed on the PPV films with the same mixing time as the DECODER spectra, but without a sample flip, indicated no molecular reorientation on this time scale, which would otherwise interfere with the interpretation of the DECODER spectra. In addition, a DECODER experiment where the sample was flipped by a certain angle and then flipped back to its start position, yielded spectral intensity along the diagonal of the 2D plane only, indicating that the sample flip mechanism was working properly.

### 2.3. PPV Chemical Shift Values

As a result of the tensorial nature of the chemical shift interaction, solid-state  $^{13}\text{C}$  NMR frequencies depend on the orientation of the  $^{13}\text{C}$  nuclei with respect to an applied external magnetic field  $\mathbf{B}_0$ ; this orientation dependence is given by [26]

$$\omega_{\text{aniso}}(\vartheta, \varphi) = \frac{1}{2}\delta(3 \cos^2 \vartheta - 1 - \eta \sin^2 \vartheta \cos(2\varphi)), \quad (1)$$

where  $(\vartheta, \varphi)$  are the polar angles of the laboratory  $\mathbf{B}_0$  field in the principal axes system (PAS) of the chemical shift tensor with components  $\sigma_{\alpha\alpha}^{\text{PAS}}$  ( $\alpha = x, y, \text{ or } z$ ). With  $\omega_\alpha = -\omega_0 \sigma_\alpha = -\omega_0(\sigma_{\alpha\alpha}^{\text{PAS}} - \sigma_{\text{iso}})$  and with the isotropic chemical shift given as  $\sigma_{\text{iso}} = (1/3)(\sigma_{xx}^{\text{PAS}} + \sigma_{yy}^{\text{PAS}} + \sigma_{zz}^{\text{PAS}})$ , the anisotropy parameter,  $\delta$ , is defined as

$$\delta = \omega_z, \quad (2)$$

and the asymmetry parameter,  $\eta$ , is defined as

$$\eta = \frac{(\omega_y - \omega_x)}{\omega_z}. \quad (3)$$

The anisotropy and asymmetry parameters are specific for every site in the molecule [11]. The Spiess–Haerberlen convention stipulates that  $|\omega_y| \leq |\omega_x| < |\omega_z|$  [34, 35], which ensures that  $0 \leq \eta \leq 1$ . For  $\eta = 0$ , the  $\mathbf{Z}_P$ -axis will always be the unique principal axis, regardless of the sign of  $\delta$ .

For the analysis and the simulation of the experimental DECODER  $^{13}\text{C}$  NMR spectra, it is necessary to know the chemical shift tensor values and the orientations of these tensors in the molecular frame for each unique site in the molecule. The structure of the repeat unit of poly(*p*-phenylene vinylene) as given in Fig. 2 reveals eight carbon atoms in PPV, several pairs of which share similar environments.

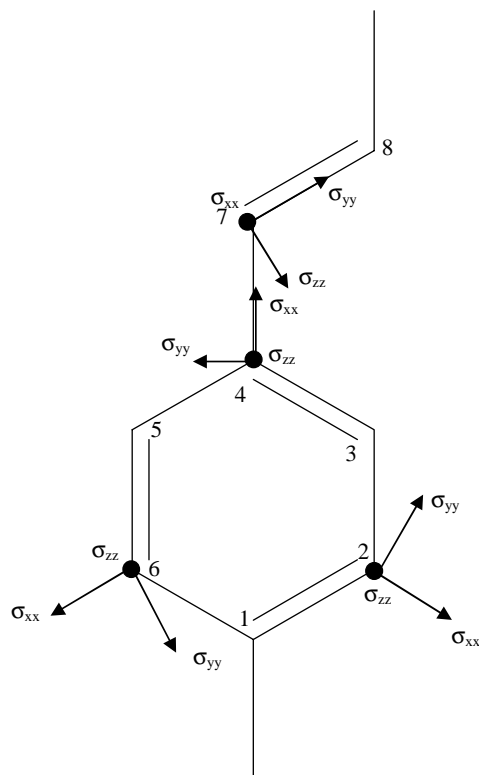


**FIG. 2.** The orientations of the principal axes systems (PAS) of the  $^{13}\text{C}$  chemical shift tensor for one carbon atom of each pair of distinct  $^{13}\text{C}$  sites in PPV. The arrows indicate the directions of the axes in the plane, while the black dots indicate axes that are normal to and out of the plane of the paper.

Previous studies have established that PPV chains have an all-*trans* configuration, due to the *ElcB* mechanism of the thermal elimination reaction [10, 13, 15, 22]. Consistent with an all-*trans* configuration for the PPV chain,  $^2\text{H}$  NMR studies of both ring- and vinylene-deuterated PPV films have shown the crystalline structure of PPV to resemble that of *trans*-stilbene [23, 36]. Consequently, the following four pairs of carbon sites yield NMR signals that are overlapping and unresolved in solid-state  $^{13}\text{C}$  NMR spectra:  $\text{C}_1$  and  $\text{C}_4$ ,  $\text{C}_2$  and  $\text{C}_5$ ,  $\text{C}_3$  and  $\text{C}_6$ , and  $\text{C}_7$  and  $\text{C}_8$ . Due to the all-*trans* configuration of the PPV chain [10, 13, 15, 22], both  $\text{C}_2$  and  $\text{C}_5$  are in a *trans* position with respect to the vinyl group, while both  $\text{C}_3$  and  $\text{C}_6$  are in a *cis* position with respect to the vinyl group. These distinct positions with respect to the vinyl group result in different isotropic chemical shifts for these two pairs of carbon sites, leading to observed frequency differences between the two pairs of protonated aromatic carbons ( $\text{C}_2$  and  $\text{C}_5$ ,  $\text{C}_3$  and  $\text{C}_6$ ). Previous solid-state  $^{13}\text{C}$  NMR studies have determined the isotropic  $^{13}\text{C}$  chemical shifts of the different carbon sites in PPV to be 136, 131, 125, and 128 ppm for  $\text{C}_{1,4}$ ,  $\text{C}_{2,5}$ ,  $\text{C}_{3,6}$ , and  $\text{C}_{7,8}$ , respectively [37–39].

In addition to measuring the isotropic  $^{13}\text{C}$  chemical shift values, Simpson *et al.* performed a Herzfeld–Berger analysis to determine the chemical shift tensor values

TABLE 1  
Chemical Shift Tensor Values for the Four Distinct Carbon Sites in PPV

$^{13}\text{C}$ site	$\sigma_{\text{iso}}$ (ppm)	$\sigma_{xx}^{\text{PAS}}$	$\sigma_{yy}^{\text{PAS}}$	$\sigma_{zz}^{\text{PAS}}$	$\eta$	$\sigma_x$	$\sigma_y$	$\sigma_z = \delta$
1,4	136	220	170	18	0.47	84	34	- 118
2,5	131	223	144	26	0.75	92	13	- 105
3,6	125	217	138	20	0.75	92	13	- 105
7,8	128	44	126	214	0.95	- 84	- 2	86
<i>trans</i> -stilbene	128	49	120	215	0.82	- 79	- 8	87
av	128	200	161	23	0.37	72	33	- 105

Note. For comparison with sites  $C_7$  and  $C_8$ , the chemical shift tensor values for the vinylene carbon sites in *trans*-stilbene are also included. The last row denoted “av” lists the chemical shift tensor values that result from a rapid  $180^\circ$  flip around the phenylene 1,4-axis, averaging the chemical shift tensor of sites 2 and 6 and sites 3 and 5.

for the four distinguishable types of carbon sites in PPV [39]. The values for  $\sigma_{xx}^{\text{PAS}}$  and  $\sigma_x (= \sigma_{xx}^{\text{PAS}} - \sigma_{\text{iso}})$  are presented in Table 1, together with the values for the isotropic  $^{13}\text{C}$  chemical shifts and the asymmetry parameters,  $\eta$ , for each resolved site. For the unprotonated phenylene sites, the chemical shift tensor values reported by Simpson *et al.* do not add to the reported isotropic chemical shift value of 136 ppm, but rather yield a value of 140 ppm instead [39]. From our DECODER experiments and simulations, we estimated the value for  $\sigma_{zz}$  to be 18 ppm, as opposed to 30 ppm, as reported previously [39]. The  $^{13}\text{C}$  tensor values listed in Table 1 for the protonated carbons in the aromatic ring are similar to those for aromatic sites in other polymers (for example, poly(ethylene terephthalate)) [28]. The values obtained for the vinyl carbons differ from values determined for polyacetylene. This discrepancy is attributed to an overlapping contribution to the  $^{13}\text{C}$  signal with the isotropic chemical shift at 128 ppm from a population of phenyl rings that are undergoing fast  $180^\circ$  flips around the 1,4-axis; this results in an average  $^{13}\text{C}$  chemical shift tensor with an isotropic shift value of 128 ppm as well, see Table 1 [39]. By analyzing  $^2\text{H}$  and  $^{13}\text{C}$  CPMAS line shapes, Simpson *et al.* determined that between 15% and 40% of the phenylene rings in their PPV sample were flipping at a rate greater than  $3.0 \times 10^3 \text{ s}^{-1}$  at ambient temperature [39, 40]. In our DECODER experiments of unstretched and stretched PPV films, we do not observe a significant NMR signal contribution from these rapidly flipping phenylene rings. This is likely due to their expected short  $T_1$  relaxation times and consequently fast signal decay during the rather long mixing times utilized in the 2D experiments.

For illustration purposes, Figs. 3a–d display simulated  $^{13}\text{C}$  NMR “powder” spectra for the chemical shift tensor values reported in Table 1; the motionally averaged spectrum resulting from the rapidly flipping phenyl rings has been omitted. For comparison, the experimental “powder” spectrum for an isotropic PPV sample is shown in Fig. 3e, while Fig. 3f displays the equally weighted sum of the simulated spectra for the four distinct sites in PPV. Also included in Figs. 3a–d are the single line spectra that would result from a perfectly oriented PPV sample for which the director axis  $Z_D$  is parallel to the molecular axis  $Z_M$  and oriented parallel to the external magnetic field  $B_0$ , which is chosen as the  $Z_L$ -axis of the laboratory frame

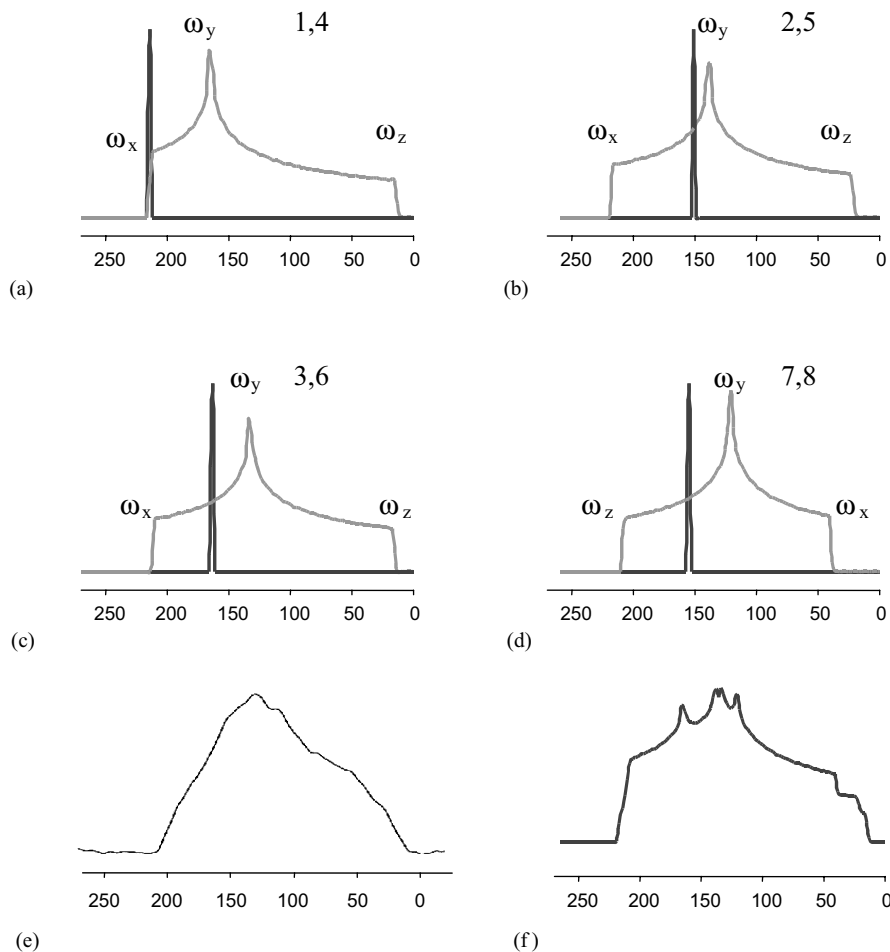


**FIG. 3.** One-dimensional simulations of  $^{13}\text{C}$  NMR powder spectra for each of the four distinct carbon sites in PPV: (a) the 1,4  $^{13}\text{C}$  sites in the phenylene ring; (b) the 2,5  $^{13}\text{C}$  sites in the phenylene ring (in the *trans*-configuration with respect to the vinylene group); (c) the 3,6  $^{13}\text{C}$  sites in the phenylene ring (in the *cis*-configuration with respect to the vinylene group); and (d) the 7,8  $^{13}\text{C}$  sites in the vinylene moieties. Superimposed on each powder spectrum are simulated  $^{13}\text{C}$  NMR line spectra that result for uniaxially drawn PPV films with all the chains perfectly aligned with respect to the draw direction; (e) the experimental “powder” spectrum of PPV; (f) the equally weighted sum of the four spectra from Figs. 3a–d.

(see below). The high degree of overlap observed in the spectrum of isotropic PPV (Fig. 3e) is not surprising, since the magnitude of the orientational dependence of the anisotropic chemical shifts in polymers is often equal to or larger than the variation in the isotropic chemical shifts of different structural units [26, 41]. As a result, only the simplest polymer structures yield powder patterns without severe overlap between powder patterns of individual carbon sites. Spectral editing techniques, such as the use of gated decoupling to suppress the signals from  $^{13}\text{C}$  moieties with directly

bonded protons or short contact times to cross-polarize selectively the protonated carbon sites, have proven inefficient to simplify the PPV spectra. The strongly overlapping spectra of the four distinct sites in PPV present challenges to the DECODER experiments and analyses of the PPV films, compared to previous DECODER studies, for example, of PET [28].

#### 2.4. PPV Chemical Shift Tensor Orientations

The orientations of the  $^{13}\text{C}$  chemical shift tensors in the molecular frame of reference must also be specified for the subsequent DECODER analysis. For aromatic carbon atoms in typical organic compounds, the tensor orientations do not vary substantially [26, 41]. Their  $\sigma_{zz}$ -axis orientation, which corresponds to the upfield (lower ppm) value,  $\omega_z$ , in the NMR powder spectrum, is taken to be normal to the plane of the phenyl ring, while the  $\sigma_{xx}$ -axis orientation that corresponds to the downfield (higher ppm) value,  $\omega_x$ , is parallel to either the C–H bond or the radial C–C bonds [39]. For the vinyl carbon sites, the tensor orientations are assumed to be similar to those in *trans*-stilbene, due to the very close similarities in their chemical structures. Thus, the downfield principal axis ( $\sigma_{xx}$ ) is perpendicular to the plane of the vinylic C=C bond, while  $\sigma_{yy}$  is parallel to the C=C double bond, and  $\sigma_{zz}$  is in the plane of the C=C double bond and perpendicular to both  $\sigma_{xx}$  and  $\sigma_{yy}$  [42]. More precisely, the orientation of  $\sigma_{zz}$  forms an angle of  $85^\circ \pm 5^\circ$  with respect to the  $^{13}\text{C}$ – $^{13}\text{C}$  internuclear vector (and hence the C=C double bond), which, in turn, results in an angle of  $5^\circ \pm 5^\circ$  for the orientation between C=C and  $\sigma_{yy}$ . The orientations for each carbon site in PPV are illustrated in Fig. 2, and the Euler angles  $\alpha_p$  and  $\beta_p$  for the transformation from the chemical shift tensor principal axes systems into the molecular frame (see below) for the four distinct  $^{13}\text{C}$  sites are summarized in Table 2.

#### 2.5. Relevant Coordinate Systems in DECODER NMR on Uniaxially Oriented Polymers

As expressed by Eq. (1), the measured solid-state NMR frequencies depend on the orientations of the  $\mathbf{B}_0$  field and the PAS of each site. When determining the orientational order of a sample, it is generally more useful to consider the orientations of the molecular chain axes with respect to a macroscopic director (as established, for example, by the draw direction). Hence, the PAS needs to be related to a molecular frame of reference, whose orientation with respect to the draw direction needs to be specified as well. The relations between these relevant coordinate systems are illustrated in Fig. 4 and are discussed below [26, 30]:

1. *Laboratory frame, LF.* The  $\mathbf{B}_0$  field defines the z-axis of the laboratory frame,  $\mathbf{Z}_L$ .
2. *Sample-fixed director frame, DF.* The z-axis of the director frame,  $\mathbf{Z}_D$ , is usually defined as the primary direction of order in the macroscopic sample, the sample director, which is the draw direction for the uniaxially stretched films discussed in this study. The polar coordinates  $(\beta_k, \alpha_k)$ ,  $k = 1, 2$ , describe the orientation of the  $\mathbf{B}_0$  field in the sample director frame during either the evolution ( $k = 1$ ) or detection ( $k = 2$ ) periods of the DECODER experiment. The two orientations of  $\mathbf{B}_0$  are separated by  $\beta_f$ , the angle through which the sample is flipped during the

TABLE 2

Euler Angles  $\alpha_p$  and  $\beta_p$  for the Transformation of the Principal-Axes Systems (PAS) of the Chemical Shift Tensors for the Four Distinct Carbon Atoms in PPV into the Molecular Frame

$^{13}\text{C}$ site	$\alpha_p$	$\beta_p$	$\alpha_p$	$\beta_p$
1	180	90	172	90
			188	90
4	0	90	352	90
			8	90
2	120	90	112	90
	240	90	248	90
5	300	90	292	90
	60	90	68	90
3	60	90	52	90
	300	90	308	90
6	240	90	232	90
	120	90	128	90
7	90	[132,142]	90	[124,134]
8	270	[48,38]	270	[56,46]

Note. The Euler angles  $\alpha_p$  and  $\beta_p$  correspond to the azimuthal and polar angles of the molecular frame  $Z_M$ -axis in the PAS, respectively. The Euler angles for the transformation of the average chemical shift tensor resulting from the rapidly flipping phenylene rings into the molecular frame are identical to the angles given for carbon sites  $C_1$  and  $C_4$ . The set of angles in the first and second columns corresponds to the choice of the molecular axis along the *para*-axis of the phenylene rings, whereas the set in the third and fourth columns is for a structure where the molecular  $Z_M$ -axis forms an angle of  $8^\circ$  with the *para*-axis of the phenylene rings. For the  $C_7$  and  $C_8$  chemical shift tensor orientations, a range is given corresponding to the interval  $[80^\circ, 90^\circ]$  for the orientation of the  $\sigma_{zz}$ -axis with respect to the  $\text{C}=\text{C}$  double bond. The other entries in each cell represent equivalent sets of Euler angles that leave the NMR frequency unchanged and which correspond to either the second carbon atom in each pair of equivalent atoms in PPV or to an equivalent choice of the PAS orientation.

DECODER experiment about the flip axis,  $F$ . When performing a DECODER NMR experiment on uniaxially stretched polymer films, the sample preparation required to flip the sample around any of the three DF coordinate axes is relatively easy. Because the PPV films under investigation were stretched uniaxially, it is beneficial for the main order direction of the sample,  $Z_D$ , to be oriented parallel to the laboratory  $B_0$  field during  $t_2$ , the detection period, as this orientation results in minimal spectral overlap, particularly for highly ordered samples (see Figs. 3a–d). When  $Z_D$  is perpendicular to the flip axis,  $F$ , a flip angle of  $45^\circ$  provides maximum angular resolution. When  $Z_D$  is parallel to the flip axis, a flip angle of  $90^\circ$  is preferred, because it also provides for minimal spectral overlap [26, 28]. Note that  $\beta_f = \beta_2 - \beta_1$  only if  $Z_D$  is perpendicular to the rotation axis; for  $Z_D$  oriented along the flip axis,  $\beta_f = \alpha_2 - \alpha_1$ .

3. *Molecular frame, MF*. The  $z$ -axis of the molecular frame,  $Z_M$ , is typically defined as the molecular chain axis. The orientation of the molecular frame MF with respect to the sample-fixed director frame DF is given by the Euler angles  $(\Psi_M, \Theta_M, \Phi_M)$ , of which only  $\Theta_M$  is of relevance in a uniaxially oriented sample. These Euler angles are generally more meaningful for describing the orientational order

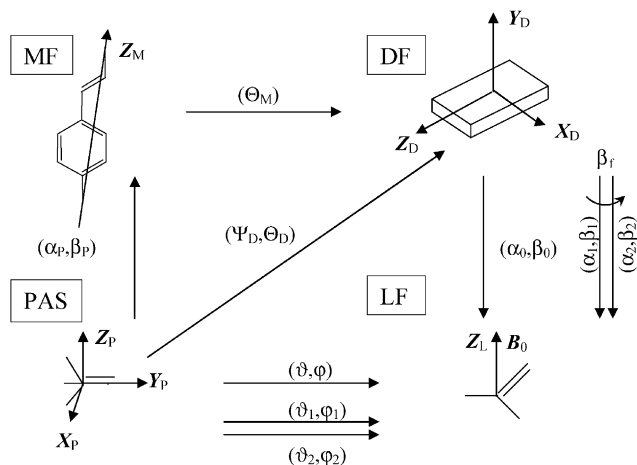


**FIG. 4.** Relationships among the coordinate systems that are relevant to the DECODER experiment, along with the angles that relate them and that are relevant to uniaxially oriented systems with transverse isotropy. “PAS” refers to the principal axes system of a given chemical shift tensor, which is specific to each site in the repeat unit. For  $\eta = 0$ , the  $Z_P$ -axis is the unique axis of the chemical shift tensor. “MF” represents the molecular frame, with the  $Z_M$ -axis defined as the polymer chain axis. “DF” corresponds to the sample director frame, with the  $Z_D$ -axis parallel to the primary order direction in the sample, e.g., the draw direction. “LF” refers to the laboratory frame, with the  $Z_L$ -axis parallel to the laboratory  $B_0$  field.

within a sample than the angles  $(\Psi_D, \Theta_D, \Phi_D)$  that relate the PAS and the DF, though  $(\Psi_D, \Theta_D, \Phi_D)$  are more directly related to the measured NMR frequencies. For uniaxial systems, only  $\Theta_D$  and  $\Psi_D$  are relevant, because transverse isotropy dictates that all orientations  $\Phi_D$  are present with equal probability.

4. *Principal-axes system, PAS.* As discussed previously, the principal-axes system for a given site is defined as the coordinate system in which the chemical shift tensor is diagonal. The polar coordinates of the  $B_0$  field in the principal axes system are given by  $(\vartheta_1, \varphi_1)$  during the evolution period and by  $(\vartheta_2, \varphi_2)$  during the detection period. The orientation of a specific PAS in the sample-fixed director frame is given by the Euler angles  $(\Psi_D, \Theta_D)$ , while its orientation in the molecular frame is specified by the Euler angles  $(\alpha_p, \beta_p, \gamma_p)$ . Both  $\gamma_p$  and  $\Psi_M$  describe rotations about the  $Z_M$ -axis in the transformation from PAS  $\rightarrow$  MF  $\rightarrow$  DF, so that it is possible to set  $\gamma_p = 0$  without restricting the treatment [26, 28].

As already mentioned above, for the case of uniaxially stretched polymers for which the conditions of transverse isotropy (macroscopic and microscopic uniaxiality) are fulfilled, the orientation distribution can be characterized in terms of  $\Theta_M$  alone [26, 28]. The definition of transverse isotropy dictates that all  $\Psi_M$  and  $\Phi_M$  are present with equal probabilities, and thus their roles in the orientation distribution are fully specified. The condition for  $\Phi_M$  is equivalent to macroscopic

uniaxiality, i.e., the distribution of the molecules or chains with respect to the sample director  $\mathbf{Z}_D$  is cylindrically symmetric. The microscopic condition for  $\Psi_M$  is usually met on the basis of fiber symmetry, for which equal probabilities of all values for  $\Psi_M$  for a rotation around the molecular chain axis is expected for a set of parallel chain axes  $\mathbf{Z}_M$ . Microscopic uniaxiality is also assured in the case of  $\eta = 0$ . In that case, with the molecular axis  $\mathbf{Z}_M$  chosen parallel to the unique principal axis  $\mathbf{Z}_P$ , different values of  $\Psi_M$  are not distinguishable because a rotation around  $\mathbf{Z}_P$  leaves the NMR frequency, and therefore the NMR spectrum, invariant [26, 28].

Three approaches are generally used for determining the orientation distribution  $P(\Theta_M)$  from experimental NMR spectra: (1) direct reconstruction, (2) assumption of a suitable functional form for  $P(\Theta_M)$  and determination of its parameters from a line shape fit, and (3) expansion of  $P(\Theta_M)$  and determination of the expansion coefficients (order parameters, moments) [30]. Out of these three approaches, the third is the most widely applied. While it is suitable for moderately ordered systems, it fails for highly ordered systems because the moment expansion converges poorly. The second method is the appropriate choice for highly ordered systems. The first method is useful for characterizing  $P(\Theta_M)$  in oriented samples over a broad range of orientational order, particularly for poorly or moderately ordered systems. It requires high-quality multidimensional data provided by the DECODER NMR experiment. 2D DECODER spectra contain information on the two Euler angles that relate the orientation of molecular segments to the primary order direction of the sample, for example, the draw direction in uniaxially drawn films. For  $\eta = 0$  spectra (in practice  $\eta \leq 0.3$ ) and non-overlapping NMR signals, the intensity distribution of a 2D DECODER spectrum directly reflects the orientation distribution, and it is possible to reconstruct conveniently and reliably the orientation distribution directly from the experimental spectra. The case of  $\eta \leq 0.3$  and parallel orientation of the molecular and principal axis,  $\mathbf{Z}_M \parallel \mathbf{Z}_P$ , which renders  $\Theta_M = \Theta$  and which was observed for the  $\text{OCH}_2$  and carboxyl groups in PET [28], is not met for any of the four distinct  $^{13}\text{C}$  sites in PPV. Thus, it is not possible to make a direct reconstruction of the orientation distribution from the 2D  $^{13}\text{C}$  DECODER spectra. For  $\eta \neq 0$ , the orientation of every PAS in the sample fixed frame (DF) must be specified, requiring the specification of three angles that can be established only by measuring the NMR frequency at least three times, for instance in a 3D DECODER experiment. In view of the already very long acquisition times of 2D DECODER spectra for the PPV films, a 3D DECODER experiment was not considered feasible. Although the degree of orientational order is directly reflected by the spread of the spectral intensity in a 2D DECODER NMR spectrum even for  $\eta \neq 0$ , as is the case for all of the different sites in PPV, computer simulations are required to determine estimates of the orientation distribution [7]. The DECODER NMR spectra simulations were performed using FORTRAN programs and were used to determine the fwhm of a Gaussian-shaped orientation distribution by visual comparison with the experimental DECODER spectra. It is then possible to calculate order parameters  $\langle P_L \rangle$  for high values of  $L$  from a moment expansion of the so-determined Gaussian distributions; as magnetic resonance frequencies are governed by second-rank tensors, only the higher-order moments for even  $L$  are accessible.

### 3. RESULTS AND DISCUSSION

#### 3.1. 1D NMR Spectra of Oriented and Uniaxially Drawn PPV Films

Conventional static 1D solid-state  $^{13}\text{C}$  NMR spectra in Fig. 5 of unstretched ( $\lambda = 1$ ) films and stretched films ( $\lambda = 5$ ) PPV films give an indication of the degree of orientational order present in these films. Such spectra were acquired with the draw directions of the films either perpendicular (Figs. 5a and 5b) or parallel (Figs. 5c and 5d) to the  $B_0$  field, using an identical number of data accumulations; the signal-to-noise ratios in Figs. 5b and 5d are lower than those in Figs. 5a and 5c, respectively, because less sample was available for the stretched films. These static 1D  $^{13}\text{C}$  NMR spectra illustrate that some degree of orientational order is present in the unstretched films, as established by clear differences in the spectra at the two orientations with respect to the external magnetic field  $B_0$ , both of which are distinct from the experimental spectrum of an isotropic PPV sample (Fig. 3e). It is evident, however, that the degree of orientational order is significantly higher in the stretched films, in

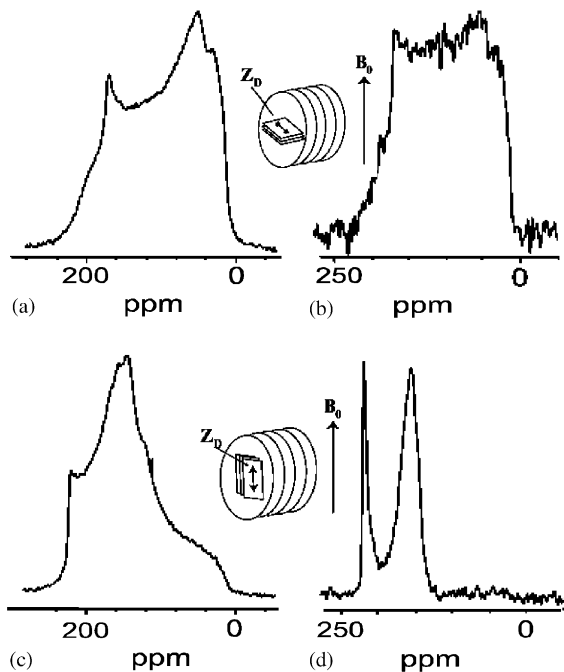


**FIG. 5.** One-dimensional  $^{13}\text{C}$  NMR spectra of unstretched (a and c) and cold-stretched (b and d) PPV films with the draw direction of the films oriented perpendicular (a and b) and parallel (c and d) to the external magnetic field  $B_0$ . The spectra of the unstretched PPV film (a and c) demonstrate that orientational order is present even in these unstretched films (compare to Fig. 3e for the spectrum of an isotropic PPV sample). In particular, the narrow lines in the spectrum of the stretched PPV film that is oriented with the draw direction parallel to the  $B_0$  field (d) indicate the high degree of molecular ordering achievable by cold-stretching the PPV precursor films (compare to the simulated line spectra in Figs. 3a–d.)

particular, because of the very narrow spectral patterns in Fig. 5d. For this particular orientation of the PPV film, with  $\mathbf{B}_0$  oriented in the film plane and parallel to the sample director, the spectral intensities for the carbon atoms (2, 5), (3, 6), and (7, 8) are concentrated near the  $\omega_y$  value of their corresponding powder patterns, indicating that the  $\sigma_{yy}$  principal axis of their respective chemical shift tensors is oriented close to the  $\mathbf{B}_0$  field direction, see Fig. 2. Note that this condition does not imply that phenylene rings in different chains have to be oriented parallel with each other; cylindrical symmetry is sufficient. Similarly, for carbon sites (1, 4) the intensity is mainly found near the downfield  $\omega_x$  value, indicating that in this case the  $\sigma_{xx}$ -axis of the chemical shift tensor is oriented close to the  $\mathbf{B}_0$  field direction. The frequency position of this particular line indicates that the angle the 1,4 or *para*-axis of the phenylene rings forms with the molecular axis  $\mathbf{Z}_M$  and the director axis  $\mathbf{Z}_D$  must be a small one. To clarify this, the 1D  $^{13}\text{C}$  line spectra for a perfectly ordered PPV sample are overlaid on the simulated powder spectra shown in Figs. 3a–d. In perfectly ordered uniaxial samples, the polar coordinates ( $\Theta_D, \Psi_D$ ) of the sample director  $\mathbf{Z}_D$  in the PAS are the same for all equivalent sites in the polymer chain (i.e., the polar coordinates for  $\mathbf{Z}_D$  will be the same in the PAS for all  $\text{C}_1$  sites in a perfectly ordered sample.) Because  $\mathbf{B}_0$  is parallel to  $\mathbf{Z}_D$  in this orientation,  $\mathbf{B}_0$  has the same polar coordinates in the principal-axes systems ( $\vartheta = \Theta_D, \varphi = \Psi_D$ ) as  $\mathbf{Z}_D$ . As a result, all the equivalent sites have the same frequency  $\omega(\vartheta, \varphi)$ , resulting in the sharp spectral patterns [26].

### 3.2. DECODER $^{13}\text{C}$ NMR Studies of Oriented and Uniaxially Drawn PPV Films

To familiarize the reader with the appearance of DECODER  $^{13}\text{C}$  NMR spectra, Figs. 6a–d display simulated DECODER spectra for the two extreme cases of perfectly uniaxially oriented samples with transverse isotropy (Figs. 6a and 6c) and of isotropic samples (Figs. 6b and 6d). These spectra were calculated for sample flips with the flip axis either parallel to  $X_D$  and  $Y_D$  (Figs. 6a and 6b), which are indistinguishable for transverse isotropic samples, or parallel to the  $Z_D$ -axis (Figs. 6c and 6d), and for flip angles  $\beta_f = 45^\circ$  and  $90^\circ$ , respectively, using the tensor values for PPV as given in Table 1 and assuming equal intensities for the spectral contributions from each of the four distinct sites. For simplicity, it was assumed that the vinyl linkage and the phenylene rings are in the same plane. Simulations that include a small dihedral angle between the plane of the phenylene rings and the plane of the vinylene linkage, which was found to be  $10^\circ \pm 3^\circ$  at room temperature by X-ray diffraction [14] and  $7^\circ \pm 6^\circ$  by elastic neutron scattering [19], do not lead to significant modifications in the line shapes displayed here.

Simpson *et al.* determined from  $^2\text{H}$  NMR line shape analyses that, on average, the *para*-axis of the phenylene ring forms an angle of  $7.7^\circ \pm 0.5^\circ$  with respect to the molecular chain axis [23], whereas in *trans*-stilbene, this angle was found to be  $9.2^\circ$  [42]. For the simulations in Fig. 5, a tilt angle of  $8^\circ$  was used. Perfect  $120^\circ$  bond angles were assumed for the orientations of the C–H bonds and the C–C bonds of the phenylene rings. In accordance with a value of  $85^\circ \pm 5^\circ$  determined for the angle between the  $\sigma_{zz}$ -axis of the vinylene carbons and the C=C double bond, a value of  $85^\circ$  degrees was used in the simulation, and the C–C=C angle was assumed to be  $128^\circ$  [14, 18]. The line shapes resulting from the portion of the phenylene rings

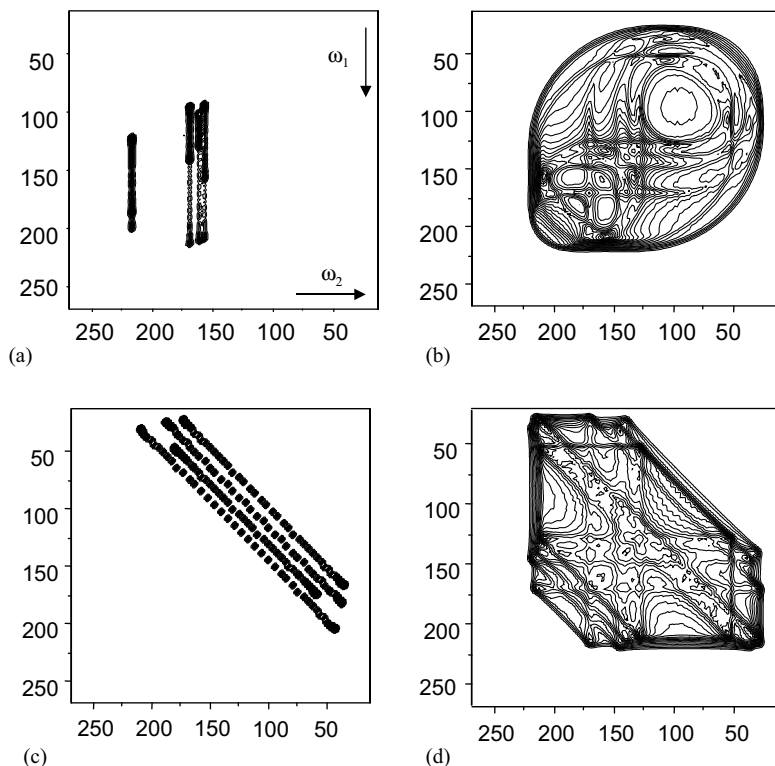


**FIG. 6.** Simulated DECODER  $^{13}\text{C}$  NMR spectra for PPV, assuming idealized conditions, including the absence of rapid phenylene ring motions. The simulations for perfect order are on the left, while the “powder” spectra are on the right. The two spectra in (a) and (b) are calculated for a  $45^\circ$  flip about the flip axis  $F$ , which is aligned parallel to the director frame axis  $X_D$  (or equivalently  $Y_D$  for oriented samples with transverse isotropy.) Furthermore, the sample director was chosen to coincide with the external magnetic field direction during the detection period of the DECODER experiment, resulting in narrow spectral lines in the  $\omega_2$  dimension (compare to the line spectra in Figs. 3a–d). The spectra in (c) and (d) were simulated for a  $90^\circ$  flip about the flip axis  $F$ , which is aligned parallel to  $Z_D$ . These experimental conditions are especially suited to reduce spectral overlap between signals from different  $^{13}\text{C}$  sites. See text for further details. Note that in order to make spectral intensity positions for the four distinct carbon sites in PPV distinguishable in these spectra, no time domain signal apodization or spectral peak convolution has been applied, resulting in numerical noise being visible, particular in the spectrum (c).

undergoing rapid  $180^\circ$  flips, which leads to a motionally averaged chemical shift tensor (see Table 1) have been omitted from the simulation for clarity.

The simulations for the DECODER reorientation of isotropic PPV samples (Figs. 6b and 6d) reflect the characteristic elliptical features for reorientation by a discrete flip angle [25, 26, 28]. In DECODER NMR, even for  $\eta \neq 0$ , elliptical patterns (which are also characteristic for  $\eta = 0$ ) are observed, though they appear as three-fold overlapping features in powder spectra. For a flip angle of  $45^\circ$ , these ellipses become circles, and for  $90^\circ$  they collapse into single straight lines. The smallest ellipse touches the frequency positions  $\omega_x$  and  $\omega_y$  in both dimensions, the largest one

touches  $\omega_x$  and  $\omega_z$ , and the intermediate one abuts  $\omega_y$  and  $\omega_z$ . Concerning the extension of the patterns in the frequency plane, note in particular that the corners  $(\omega_x, \omega_x)$  and  $(\omega_z, \omega_z)$  are not accessible for  $\beta_f \neq 0$  and  $\eta \neq 0$ . The observation of spectral intensity at these frequency positions would require the  $\mathbf{B}_0$  field to be aligned parallel with the corresponding axes of the chemical shift tensor during both the evolution and detection period, which is impossible, since the sample is rotated around an axis perpendicular to  $\mathbf{B}_0$ . The powder spectrum contains contributions from all possible orientations; its boundaries therefore represent the outermost limits for the 2D DECODER spectrum of any partially ordered sample.

The two DECODER spectra shown in Figs. 6a and 6c are calculated for the two important cases for an uniaxially ordered sample discussed above: (i) a  $45^\circ$  flip with the order axis  $\mathbf{Z}_D$  perpendicular to the flip axis  $\mathbf{F}$  for maximum angular resolution and along with the order axis being parallel to  $\mathbf{B}_0$  during the detection period to minimize spectral overlap, and (ii) a  $90^\circ$  flip with the order axis parallel to the flip axis  $\mathbf{F}$  for minimal spectral overlap. In the first case, the sample director is assumed to coincide with the molecular axis and is oriented parallel to the external magnetic field, as is the case during the detection period for the spectrum displayed in Fig. 6a. The projection of the 2D signal intensity onto the  $\omega_2$  dimension yields a simulated 1D spectrum very similar in appearance to the experimental  $^{13}\text{C}$  NMR spectrum for stretched PPV shown in Fig. 5d: essentially four sharp lines parallel to the  $\omega_1$  dimension for the four distinct sites in PPV. Of these, the line farthest downfield can be assigned to the unprotonated carbon sites in the phenylene rings, for which the  $\sigma_{xx}$ -axis is almost parallel to the molecular axis. The other three lines are very close together; their absolute positions, and in particular their relative positions with respect to each other are very sensitive to the choice of the Euler angles  $\alpha_p$  and  $\beta_p$  that relate the respective PASs to the molecular axis, see Figs. 2 and 4.

In the second case, the DECODER spectrum of a uniaxially ordered sample is simulated for a  $90^\circ$  flip about the draw direction ( $\mathbf{Z}_D \parallel \mathbf{F}$ ). The simulated DECODER spectrum for this situation is shown in Fig. 6c, containing four narrow and separate lines that correspond to the four distinct  $^{13}\text{C}$  sites in PPV. For  $\mathbf{Z}_M \parallel \mathbf{Z}_D$ , that is,  $\Theta_M = 0^\circ$ , their relative positions are dictated by the Euler angle  $\alpha_p$ . On the basis of the above discussion, for narrow  $\Theta_M$  distributions around  $\Theta_M = 0^\circ$ , spectra similar to the ones depicted in Figs. 6a and 6c are to be expected. Furthermore, these simulated spectra indicate that, despite the high degree of spectral overlap observed in the 1D NMR spectra of PPV, 2D DECODER NMR spectra with resolved signal intensities from the different carbon sites are obtainable for highly ordered samples.

Figs. 7a and 7c show the experimental DECODER  $^{13}\text{C}$  NMR spectrum, both as contour and stacked plots, acquired from an oriented but unstretched PPV film for a  $45^\circ$  flip around  $\mathbf{X}_D$ . The corresponding 1D  $^{13}\text{C}$  NMR spectra of this film are presented in Figs. 5a and 5c. It is evident from the experimental spectrum that the unstretched films do not possess a high degree of orientational order. The spectrum closely resembles that of an isotropic distribution without, however, displaying the full symmetrical ellipses that are present in the DECODER spectra for fully isotropic samples, compare Fig. 6. In the contour plot of the experimental spectrum, the dominant features are the regions of high intensity that correspond to the edges of the three-fold elliptical pattern for each distinct chemical shift tensor in PPV. In

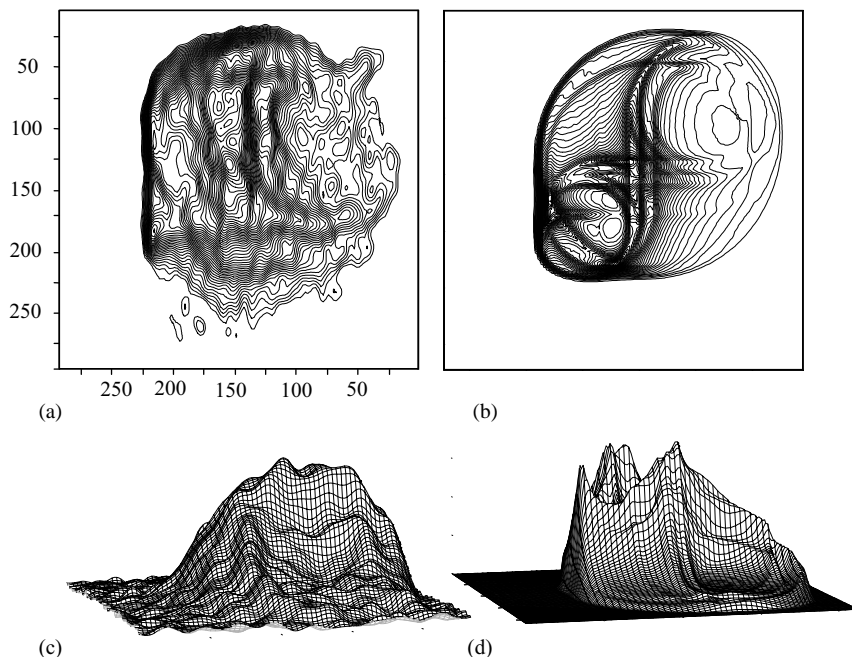


**FIG. 7.** DECODER  $^{13}\text{C}$  NMR spectra obtained for a  $45^\circ$  flip of the unstretched PPV film about the  $X_D$ -axis. The experimental DECODER spectra are shown on the left (a and c), while the simulations that best match the experimental spectra are shown on the right (b and d). It was determined that the unstretched film possesses two components: 80% of the chains are aligned about the draw direction with a fwhm of  $60^\circ$ , while the remaining 20% of the chains are isotropically distributed.

particular, the arc of the large outer ellipse around the left and top edges of the spectrum, as well as the three separate arcs of the medium-size ellipse that lie parallel to  $\omega_1$  in the upper right of the spectrum, and the arcs of the small ellipse that run parallel to  $\omega_2$  in the lower right of the spectrum are the distinct features that are reproduced well in the simulation.

The DECODER simulation that most closely matches the experimental DECODER spectrum is displayed in Figs. 7b and 7d. From comparison with simulations like the one shown in Fig. 7b, it is determined that the unstretched PPV film possesses a majority component (approximately 80% of the chains) whose chains are aligned about the draw direction with an fwhm of  $60^\circ$  (corresponding to a value for  $\langle P_2 \rangle$  of 0.564), while the remaining approximately 20% of the chains are isotropically distributed. The distribution obtained is significantly narrower than the distribution determined by Dermaut *et al.* for unstretched PPV films, where an fwhm of  $90^\circ$  ( $\langle P_2 \rangle = 0.32$ ) was found [11].

Three different DECODER experiments were performed on the stretched PPV films, the 1D  $^{13}\text{C}$  NMR spectra of which are presented in Figs. 5b and 5d. The DECODER spectrum for the stretched PPV film with a  $45^\circ$  flip around  $X_D$  is presented in Figs. 8a and 8c, while Figs. 8b and 8d show the DECODER spectrum for a  $45^\circ$  flip around  $Y_D$ . The primary features of the experimental spectra are the

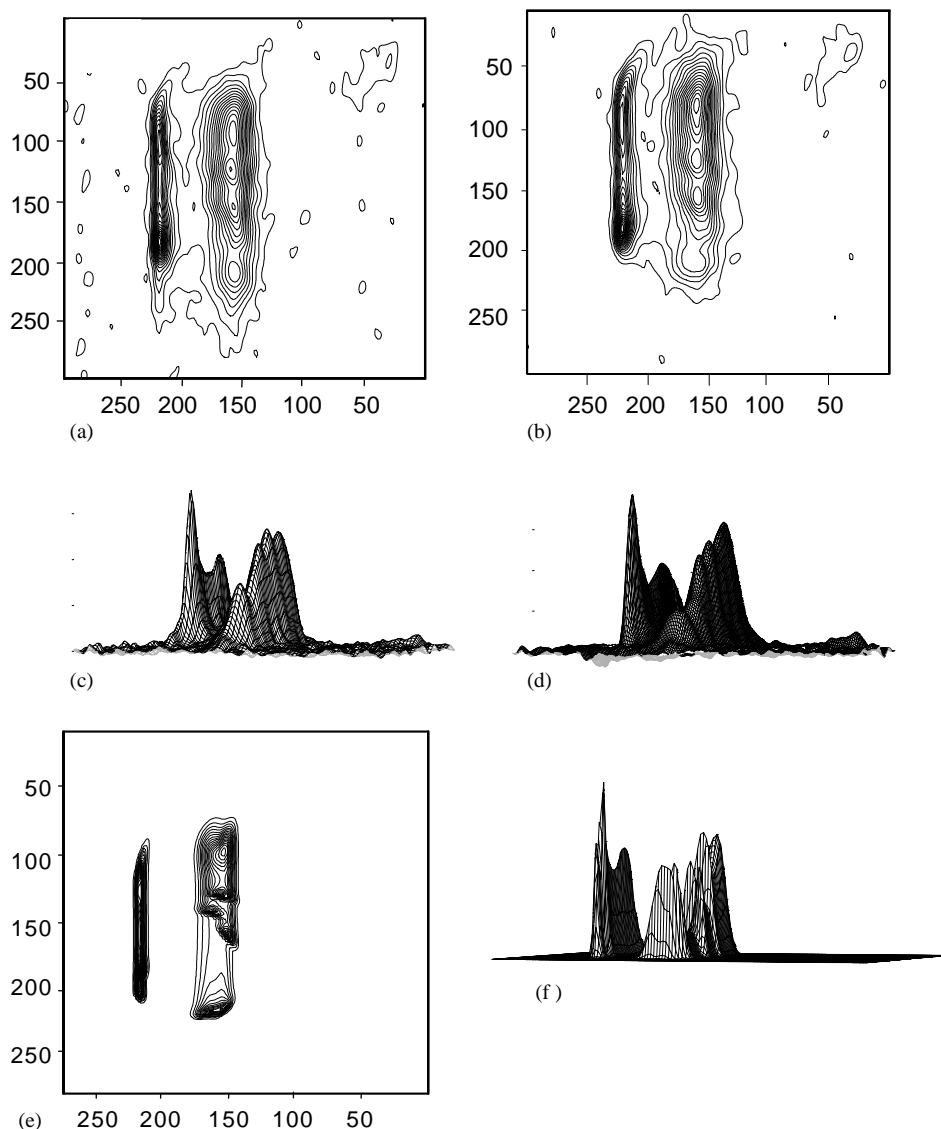


**FIG. 8.** DECODER  $^{13}\text{C}$  NMR spectra obtained for a  $45^\circ$  flip of the stretched film ( $\lambda = 5$ ) about  $X_D$  (a and c) and  $Y_D$  (b and d). There is little difference in these two spectra, as expected for a uniaxially stretched sample with transverse isotropy. The simulated DECODER spectra in (e) and (f) are calculated for a Gaussian orientation distribution with a fwhm of  $9^\circ$ . Comparison with spectra simulated for different widths of the orientation distribution provides an uncertainty estimate of  $\pm 3^\circ$ .

relatively narrow peak at  $\sim 220$  ppm in the  $\omega_2$  dimension and the superposition of several peaks near 160 ppm. There is little difference in these two spectra, as expected for a uniaxially stretched sample with transverse isotropy, which in turn validates this assumption. It is likely that the phenyl rings and vinyl linkages have a preferred

orientation within individual crystallites, and that the distribution of crystallite orientations about the draw direction results in the observed fiber symmetry. Figures 8e and 8f show the corresponding simulation for a Gaussian orientation distribution with an fwhm of  $9^\circ \pm 3^\circ$ . Smaller fwhm values result in less overlap between the upfield signals of the protonated carbons than is actually observed, while larger values cause the dip in the left peak to become filled and also the width of the pattern at the right to become too broad. For a Gaussian distribution with an fwhm of  $9^\circ \pm 3^\circ$ , the values for the Hermans orientation function or second order parameter fall within the range  $0.977 < \langle P_2 \rangle < 0.994$ . Values for  $\langle P_4 \rangle$  range from 0.92 to 0.98, and for  $\langle P_6 \rangle$  the values fall between 0.85 and 0.96. Even for the largest width of the orientation distribution that is in accordance with the experimental DECODER data,  $\langle P_{14} \rangle$  is still about 0.27. From comparison with the DECODER simulations, it was determined that  $\beta_1 = 47^\circ$  and  $\beta_2 = 2^\circ$  for the spectrum in Figs. 8a and 8c. The small variations in the spectral features in the spectrum of Figs. 8b and 8d can be attributed to the differences in the start and end positions with respect to the  $B_0$  field of the sample flip, which in this case were at angles  $\beta_1 = 50^\circ$  and  $\beta_2 = 5^\circ$ .

Figures 9a and 9c show the experimental spectrum for an intended  $90^\circ$  flip around  $Z_D$ . By comparison with simulations, it was determined that a flip angle of  $70^\circ$  more

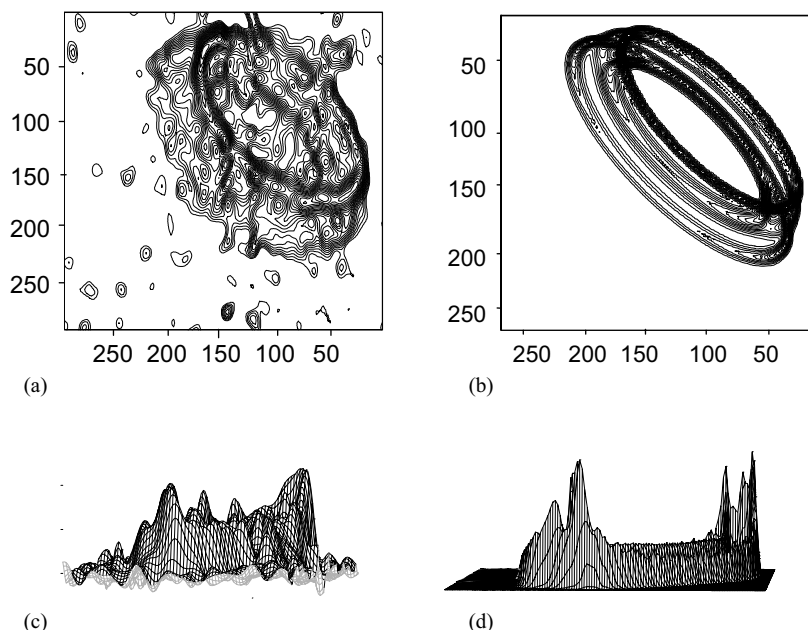


**FIG. 9.** DECODER  $^{13}\text{C}$  NMR spectra obtained for an attempted  $90^\circ$  flip about  $Z_D$ . As verified on a previously characterized PET sample, the actual flip angle is  $70^\circ$  due to limitations inherent in the sample flipping mechanism. The experimental spectrum is shown on the left (a and c) and the most closely matching simulation is shown on the right (b and d). The simulation was calculated for an fwhm of  $9^\circ$ . Because of the lower angular and spectral resolution (relative to a flip angle of  $45^\circ$ ), an error margin of  $\pm 5^\circ$  is obtained for this particular orientation of the sample with respect to the external magnetic field.

accurately reproduced the experimental results. This difference between the intended and the actual flip angle was determined to be due to a limitation inherent in the sample flip mechanism used, and was verified experimentally using a PET sample studied previously [28]. This discrepancy is only observed for large angle flips and was verified not to affect flip angles of  $45^\circ$  or smaller. For a sample flip angle  $\beta_f = 70^\circ$ , the straight lines that would be observed for a  $90^\circ$  flip (see Fig. 6c) are extended into elliptical patterns, the eccentricities of which depend solely on  $\beta_f$ . From the experimental and simulated DECODER spectra, the width (fwhm) of the distribution of PPV chain axes is determined to be  $9^\circ \pm 5^\circ$ , which is in agreement with the results obtained from the other experiments discussed above. The error margins are larger in this case, because in this configuration with the director along the sample flip axis  $F$ , it is not possible to obtain high spectral resolution during the detection period. As a result, the ratio of signal-to-noise was not as high for this experiment, as the signal is spread over a much broader region in both dimensions of the experiment.

### 3.3. Summary

This study has illustrated that natural abundance  $^{13}\text{C}$  DECODER NMR can yield useful structural information, even in the case of highly complicated and overlapping spectra. In particular, the use of DECODER NMR permitted the quantification of orientational molecular order in PPV films prepared by cold stretching. For PPV films stretched to a draw ratio of 5, a  $9^\circ \pm 3^\circ$  fwhm of a Gaussian distribution of chain axes orientations around the sample director was obtained from the DECODER analysis. In addition, for unstretched PPV films, an ordered component with a distribution fwhm of  $60^\circ$  about the draw direction was found, with an isotropic component present at approximately 20%.

Challenges to more detailed structural analysis of orientationally ordered PPV films arise in part because of the difficulty of directly reconstructing the underlying orientation distribution function, as none of the spectra corresponding to the four distinct carbon sites in PPV have asymmetry parameters lower than  $\eta \sim 0.3$ . Furthermore, overlap of signal intensities from the different  $^{13}\text{C}$  sites is severe. The different carbon sites could possibly be resolved by selectively enriching PPV with  $^{13}\text{C}$ , although such an approach is both time consuming and costly. More easily, PPV could be selectively deuterated at either the vinylene or phenyl groups so that  $^2\text{H}$  DECODER NMR could be performed, which would yield high angular resolution spectra with vanishing asymmetry parameters that could allow direct reconstruction of the full orientation distribution function. In addition, extending the natural abundance  $^{13}\text{C}$  DECODER experiment into the third dimension could help to further resolve the spectral patterns for the overlapping  $^{13}\text{C}$  sites.

## ACKNOWLEDGMENTS

This work was supported by the MRSEC Program of the U.S. National Science Foundation under Award No. DMR-0080034. W. D. thanks the Fund for Scientific Research (FWO-Vlaanderen) for a research assistant grant. We thank Professor K. Schmidt-Rohr for providing the computer code for the

DECODER simulations, Professor A. J. Heeger and his group for helpful discussions about PPV, and Dr. J. Sepa and S. R. Williams for experimental assistance. We are grateful to Professor Hans Wolfgang Spiess for his strong support of the cooperation between UCSB and the MPI in Mainz.

## REFERENCES

1. J. H. Burroughes, D. D. C. Bradley, A. R. Brown, R. N. Marks, K. Mackay, R. H. Friend, P. L. Burns, and A. B. Holmes, Light-emitting-diodes based on conjugated polymers, *Nature* **347**, 539–541 (1990).
2. W. R. Salaneck and J. L. Bredas, Conjugated polymer surfaces and interfaces for light-emitting devices, *MRS Bull.* **22**, 46–51 (1997).
3. J. J. M. Halls, K. Pichler, R. H. Friend, S. C. Moratti, and A. B. Holmes, Exciton diffusion and dissociation in a poly(*p*-phenylenevinylene)/C-60 heterojunction photovoltaic cell, *Appl. Phys. Lett.* **68**, 3120–3122 (1996).
4. N. Tessler, G. J. Denton, and R. H. Friend, Lasing from conjugated-polymer microcavities, *Nature* **382**, 695–697 (1996).
5. N. Tessler, G. J. Denton, and R. H. Friend, Lasing characteristics of PPV microcavities, *Synth. Met.* **84**, 475–476 (1997).
6. D. R. Gagnon, J. D. Capistran, F. E. Karasz, and R. W. Lenz, Conductivity anisotropy in oriented poly(*p*-phenylene vinylene), *Polym. Bull.* **12**, 293–298 (1984).
7. M. Ahlskog, M. Reghu, A. J. Heeger, T. Noguchi, and T. Ohnishi, Electronic transport in the metallic state of oriented poly(*p*-phenylenevinylene), *Phys. Rev. B* **53**, 15,529–15,537 (1996).
8. M. Ahlskog, M. Reghu, A. J. Heeger, T. Noguchi, and T. Ohnishi, Electronic transport in sulfuric acid doped poly(*p*-phenylenevinylene), *Synth. Met.* **84**, 619–620 (1997).
9. F. E. Karasz, J. D. Capistran, D. R. Gagnon, and R. W. Lenz, High molecular-weight polyphenylene vinylene, *Mol. Cryst. Liq. Cryst.* **118**, 327–332 (1985).
10. D. R. Gagnon, J. D. Capistran, F. E. Karasz, R. W. Lenz, and S. Antoun, Synthesis, doping, and electrical-conductivity of high molecular-weight poly(para-phenylene vinylene), *Polymer* **28**, 567–573 (1987).
11. W. Dermaut, T. Van den Kerkhof, B. J. van der Veken, R. Mertens, and H. J. Geise, Cold stretching of PPV with water as a plasticizer, *Macromolecules* **33**, 5634–5637 (2000).
12. H. V. Shah, J. I. Scheinbeim, and G. A. Arbuckle, Structural anisotropy in unstretched and uniaxially stretched poly(*p*-phenylene vinylene), *J. Polym. Sci. Polym. Phys.* **37**, 605–614 (1999).
13. D. R. Gagnon, F. E. Karasz, E. L. Thomas, and R. W. Lenz, Molecular orientation and conductivity in highly drawn poly(*p*-phenylene vinylene), *Synth. Met.* **20**, 85–95 (1987).
14. D. Chen, M. J. Winokur, M. A. Masse, and F. E. Karasz, A structural study of poly(*p*-phenylene vinylene), *Polymer* **33**, 3116–3122 (1992).
15. D. D. C. Bradley, R. H. Friend, T. Hartmann, E. A. Marseglia, M. M. Sokolowski, and P. D. Townsend, Structural studies of oriented precursor route conjugated polymers, *Synth. Met.* **17**, 473–478 (1987).
16. M. A. Masse, D. C. Martin, E. L. Thomas, F. E. Karasz, and J. H. Petermann, Crystal morphology in pristine and doped films of poly(*p*-phenylene vinylene), *J. Mater. Sci.* **25**, 311–320 (1990).
17. V. Massardier, V. B. Cajipe, T. P. Nguyen, and V. H. Tran, Molecular orientation in cold-stretched poly(*p*-phenylene vinylene) films, *Synth. Met.* **75**, 169–173 (1995).
18. T. Granier, E. L. Thomas, D. R. Gagnon, F. E. Karasz, and R.W. Lenz, Structure investigation of poly(*p*-phenylene vinylene), *J. Polym. Sci. Polym. Phys.* **24**, 2793–2804 (1986).
19. G. Mao, J. E. Fischer, F. E. Karasz, and M. J. Winokur, Nonplanarity and ring torsion in poly(*p*-phenylene vinylene). A neutron-diffraction study, *J. Chem. Phys.* **98**, 712–716 (1993).
20. J. Briers, W. Eevers, P. Cos, H. J. Geise, R. Mertens, P. Nagels, X. B. Zhang, G. Van Tendeloo, W. Herrebout, and B. Vanderveken, Molecular-orientation and conductivity in highly-oriented poly(*p*-phenylene vinylene), *Polymer* **35**, 4569–4572 (1994).

21. X. B. Zhang, G. Van Tendeloo, J. Van Landuyt, D. Van Dijck, J. Briers, Y. Bao, and H. J. Geise, An electron microscopic study of highly oriented undoped and  $FeCl_3$ -doped poly(*p*-phenylenevinylene), *Macromolecules* **29**, 1554–1561 (1996).
22. D. D. C. Bradley, R. H. Friend, H. Lindemberger, and S. Roth, Infrared characterization of oriented poly(*p*-phenylene vinylene), *Polymer* **27**, 1709–1713 (1986).
23. J. H. Simpson, D. M. Rice, and F. E. Karasz, Characterization of chain orientation in drawn poly(*p*-phenylene vinylene) by  $^2H$  quadrupole echo NMR spectroscopy, *Macromolecules* **25**, 2099–2106 (1992).
24. W. Dermaut, T. Van den Kerkhof, X. B. Zhang, B. Van der Veken, R. Mertens, and H. Geise, Cold stretched PPV: Molecular order in aligned precursor films, *Synth. Met.* **119**, 295–296 (2001).
25. K. Schmidt-Rohr, M. Hehn, D. Schaefer, and H. W. Spiess, Two-dimensional nuclear magnetic resonance with sample flip for characterizing orientation distributions, and its analogy to X-ray scattering, *J. Chem. Phys.* **97**, 2247–2262 (1992).
26. K. Schmidt-Rohr and H. W. Spiess, “Multidimensional Solid-State NMR and Polymers,” Academic Press, London, San Diego, 1994.
27. P. M. Henrichs, Molecular orientation and structure in solid polymers with  $^{13}C$  NMR: A study of biaxial films of poly(ethylene terephthalate), *Macromolecules* **20**, 2099–2112 (1987).
28. B. F. Chmelka, K. Schmidt-Rohr, and H. W. Spiess, Molecular orientation distribution in poly(ethylene terephthalate) thin films and fibers from multidimensional DECODER NMR spectroscopy, *Macromolecules* **26**, 2282–2296 (1993).
29. M. Wilhelm, S. F. Delacroix, J. J. Titman, K. Schmidt-Rohr, and H. W. Spiess, The orientation distribution in an industrial sample of poly(*p*-phenylene terephthalamide) determined by two- and three-dimensional NMR techniques, *Acta Polym.* **44**, 279–284 (1993).
30. I. M. Ward (Ed.), “Structure and Properties of Oriented Polymers,” 2nd ed., Chapman & Hall, New York, 1997.
31. T. Granier, E. L. Thomas, and F. E. Karasz, Paracrystalline structure of poly(para-phenylene vinylene), *J. Polym. Sci. Polym. Phys.* **27**, 469–487 (1989).
32. E. Bernabeu and J. M. Boix, Evaluation of paracrystallinity in blown polyethylene films by generalized Clausius–Mosotti equation, *Polym. Eng. Sci.* **39**, 609–616 (1999).
33. J. M. Machado, M. A. Masse, and F. E. Karasz, Anisotropic mechanical-properties of uniaxially oriented electrically conducting poly(para-phenylene vinylene), *Polymer* **30**, 1992–1996 (1989).
34. U. Haeberlen, “High Resolution NMR in Solids: Selective Averaging,” Academic Press, New York, 1976.
35. H. W. Spiess, *NMR Basic Princ. Prog.* **15**, 55 (1978).
36. J. H. Simpson, W. B. Liang, D. M. Rice, and F. E. Karasz, Solid-state  $^2H$  quadrupole NMR characterization of vinylene-deuterated poly(*p*-phenylenevinylene) films, *Macromolecules* **25**, 3068–3074 (1992).
37. J. Grobelny, J. Obrzut, and F. E. Karasz, Solid-state  $^{13}C$  NMR study of neutral insulating and electrochemically conducting poly(*p*-phenylenevinylene), *Synth. Met.* **29**, E97–E102 (1989).
38. J. Nouwen, D. Vanderzande, H. Martens, J. Gelan, Y. Zhou, and H. J. Geise, Structural assignment of conductive polymers by CP/MAS  $^{13}C$  NMR, *Synth. Met.* **41**, 305–308 (1991).
39. J. H. Simpson, N. Egger, M. A. Masse, D. M. Rice, and F. E. Karasz, Solid-state  $^{13}C$  NMR characterization of poly(*p*-phenylene vinylene) PPV films, *J. Polym. Sci. Polym. Phys.* **28**, 1859–1869 (1990).
40. J. H. Simpson, D. M. Rice, and F. E. Karasz,  $^2H$  NMR characterization of phenylene ring flip motion in poly(*p*-phenylene vinylene) films, *J. Polym. Sci. Polym. Phys.* **30**, 11–18 (1992).
41. W. S. Veeman, Carbon-13 chemical shift anisotropy, *Prog. Nucl. Magn. Reson. Spectrosc.* **16**, 193–235 (1984).
42. G. M. Bernard, G. Wu, and R. E. Wasylshen, An experimental and theoretical investigation of the olefinic carbon chemical shift tensors in *trans*-stilbene and  $Pt(\eta^2\text{-trans-stilbene})(PPh_3)_2$ , *J. Phys. Chem. A* **102**, 3184–3192 (1998).